Article published online: 2022-09-20

ORIGINAL ARTICLE

Evaluation of Technetium-99m glucoheptonate single photon emission computed tomography for brain tumor grading

Syed Shafiq Alam, Syed Junaid, Syed Mushtaq Ahmed

Department of Nuclear Medicine, Sher-I-Kashmir Institute of Medical Sciences, Srinagar, Jammu and Kashmir, India

ABSTRACT

Background: This study is designed to appraise the diagnostic value of technetium-99m glucoheptonate (Tc-99m GHA) single photon emission computed tomography (SPECT) in brain tumor grading.

Subjects and Methods: The study was performed on 30 patients referred from the Department of Neurosurgery, who were from both urban and rural areas. Data were collected through interview, history taking, and clinical examination followed by recording the desired parameters and finally imaging. The study subjects were divided into five groups: Controls ($n = 4$), low-grade tumors ($n = 8$), high-grade tumors ($n = 8$), metastases ($n = 5$), and nonneoplastic lesions ($n = 5$). This division was based on the World Health Organization (WHO) classification postclinico-histological diagnosis. Each of the subjects underwent contrast-enhanced computed tomography/contrast-enhanced magnetic resonance and Tc-99m GHA SPECT preoperatively. All were followed up postoperatively, and histopathological reports were regarded as the gold standard for tumor grading wherever available.

Results: It was found that high-grade tumors (Grades III/IV and IV/IV according to the WHO classification) showed significantly higher tumor to normal (T/N) ratios as well as T_{max}/N ratios when compared with low-grade tumors (Grades I/IV and II/IV), metastases or nonneoplastic lesions.

Conclusions: In summary, the results of this study suggest that in situations where a preoperative grading of tumor is required Tc-99m GHA can be used in tumor grading and its use should be encouraged. Semi-quantitative analysis using both T/N as well as T_{max}/N can be used in differentiating high-grade tumors from low-grade ones.

Key words: Brain tumor, glucoheptonate, grading, single photon emission computed tomography

Introduction

The brain has always remained a mystery to mankind, from philosophers to layman alike. However, the views about its structure and function have changed over the centuries. From Aristotle's view that its function was merely to cool the blood to the modern day understanding of the synaptic conduction between its 6 billion neurons, we have come a long way. However, nuclear medicine and molecular imaging have been at the forefront in helping in unraveling its functions as well as its malfunctions.[1]

Brain scanning using technetium-99m (Tc-99m) radiopharmaceuticals was started with pertechnetate in the 1960's which was replaced by Tc-99m diethlyenetriaminepentaacetic acid (DTPA), and Tc-99m glucoheptonate (Tc-99m GHA), which are well-known renal radiopharmaceuticals, devoid of the shortcomings of Tc-99m pertechnetate. Similarly, thallium-201, Tc-99m tetrofosmin, and

Access this article online	
Quick Response Code:	Website: www.asianjns.org
	DOI: 10.4103/1793-5482.177633

Address for correspondence:
Dr. Syed Junaid, House No. 749, Second Floor, Sector 69, Mohali, Punjab, India.
E-mail: syedjunaiddr@gmail.com

How to cite this article: Alam SS, Junaid S, Ahmed SM. Evaluation of Technetium-99m glucoheptonate single photon emission computed tomography for brain tumor grading. Asian J Neurosurg 2016;11:118-28.

Tc-99m sestamibi were found to delineate brain tumors which involved multiple mechanisms of uptake besides blood-brain barrier (BBB) disruption; however, their overwhelming cost and availability of morphological imaging techniques send these modalities to a back burner.[2]

There remains a large segment of patients with brain lesions who do not have access to any economic and readily available functional imaging modality which would have helped in tumor characterization and grading as well as delineating brain tumors from nonneoplastic ring enhancing lesions thereby aiding surgery or stereotactic biopsy.

Subjects and Methods

The study was conducted prospectively on 30 patients, referred from the Department of Neurosurgery. All the cases were clinico-anatomically suspected of brain tumors. They underwent a comprehensive clinical evaluation before subjecting them for imaging. A preoperative single photon emission computed tomography (SPECT) scan was acquired after a single intravenous injection of 20–25 mCi (740–925 MBq) of Tc-99m GHA.

After attenuation correction had been done on the raw data using Chang's protocol, semi-quantitative indices were calculated in all the cases which were then compared along the lines of tumor grading to find a correlation between them.[3]

Contrast-enhanced computed tomography (CECT) and/or magnetic resonance imaging (MRI) was done in all these patients and these were regarded as comparative standards in detection and grading of brain tumors. Subsequently, the patients were followed up to determine histopathology of the resected tumor which was regarded as a gold standard for confirmation of tumor origin, histology, and grading.

After acquiring all the results, a statistical significance between GHA indices and tumor grading was calculated and compared with other modalities such as CT/MRI.

Acquisition and reconstruction parameters

To perform brain Tc-99m GHA SPECT, the patients were administered 740-925 MBq (20–25 mCi) of Tc-99m GHA intravenously. Brain SPECT images were acquired 60 min postinjection using a dual head SPECT system (e.cam signature series from Siemens) fitted with a low energy all-purpose collimator after performing routine SPECT quality control procedures. The head was immobilized in a carbon fiber composite immobilizer to prevent motion artifacts. Energy settings of 140 keV with a 15% energy window were set. A 128 × 128 image matrix with 128 views every 3° for 25 s per view were obtained in a step and shoot mode with a zoom of 1.46. Reconstruction was performed using ordered subset expectation maximization with four subsets and eight iterations and using Chang's method for attenuation correction with a correction factor of 0.13.[4] Reconstructed images were displayed and analyzed using axial, coronal, and sagittal views. The counts per slice were plotted in a series region-of-interest (ROI) frame-activity curve [Figures 1 and 2] comparing the tumor area to symmetrically positioned mirror ROI to obtain quantitative ratios of tumor to normal (T/N).

Image analysis

Qualitative analysis

Two experienced nuclear medicine physicians evaluated the SPECT images independently. The images were interpreted as either showing or not showing evidence of tumor. Abnormally increased radiotracer uptake over the affected region within the brain parenchyma was considered indicative of tumor. Preferential accumulation of the tumor-seeking tracer in the tumor was defined as a lesion-to-background ratio.

Semi-quantitative analysis

Semi-quantitative analysis was performed by calculation of tumor to background ratios using user selected ROIs over the tumor as well as a contralateral mirror ROI as visualized in an axial (transverse sectional) slice. Two GHA indices were calculated T/N and T_{max}/N ratios which calculated the mean activity and maximum pixel activity between the tumor's

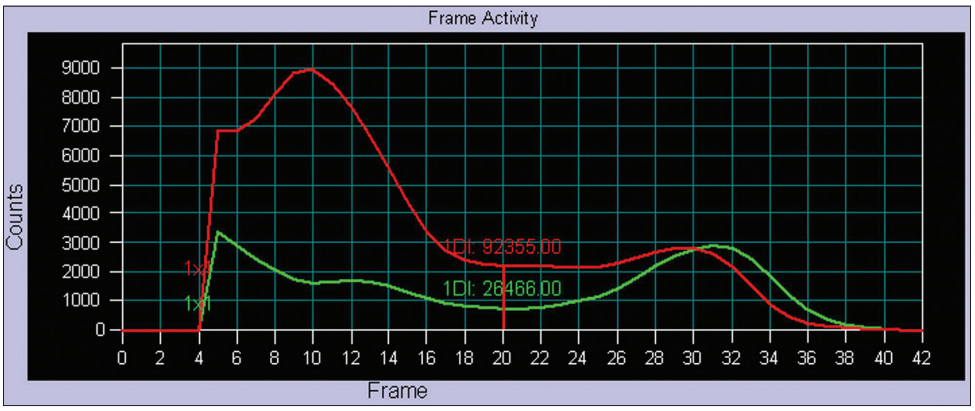

Figure 1: Frame activity curve of tumor and contralateral mirror region-of-interest

ROI to the contralateral mirror ROI, respectively which can be noted from the master table [Table 1].[5]

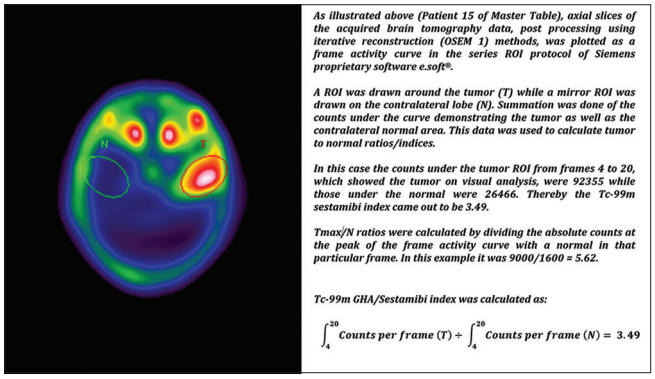

Figure 2: Calculation of tumor to normal indices

Results

Thirty subjects that were selected for the study were broadly divided into five major groups.

Group 1: It consisted of the control cases. These were either normal individuals or those suffering from an unrelated malignancy with no clinico-anatomical evidence of intracranial space occupying lesions (ICSOLs) ($n = 4$).

Group 2: It consisted of patients with World Health Organization (WHO) Grade I/II tumors ($n = 8$).

Group 3: It consisted of patients with WHO Grade III/IV tumors ($n = 8$).

Group 4: It consisted of patients with known cerebral metastases ($n = 5$).

Table 1: Master table

Patient	Age (years)	Sex	Histology	WHO grade	CT	MRI	SPECT	Location	Tumor	Normal	T/N	T_{max}/N	Outcome
1	60	Male	N (lung cancer)	Control group	–	NA	–	-	-	-	1.0	1.0	-
2	50	Male	N (lung cancer)	Control group	–	NA	–	-	-	-	1.0	1.0	-
3	60	Female	N (breast cancer)	Control group	–	NA	–	-	-	-	1.0	1.0	-
4	55	Male	N	Control group	–	NA	–	-	-	-	1.0	1.0	-
5	40	Female	Pituitary macroadenoma	I	NA	+	–	Pituitary fossa	-	-	1.0	1.0	Alive
6	38	Male	Meningioma	I	NA	+	+	Fronto-parietal	137567	83666	1.64	2.00	Alive
7	23	Female	Vestibular schwannoma	I	+	+	+	Right internal auditory meatus	1434610	821400	1.74	4.82	Alive
8	60	Male	Pilocytic astrocytoma	I	+	NA	+	Left occipital	207311	86469	2.39	2.40	Alive
9	36	Male	Oligodendroglioma	I-II	–	+	–	Left frontal	-	-	1.0	1.0	Alive
10	40	Female	Anaplastic meningioma	II	+	NA	+	Right fronto-parietal	140556	82680	1.70	2.01	Died
11	35	Male	Oligodendroglioma	I-II	NA	+	+	Left parietal	139780	66562	2.1	2.4	Alive
12	30	Male	Diffused astrocytoma	II	NA	+	+	Right medial temporal	185653	100525	1.85	2.10	Alive
13	50	Male	Anaplastic oligodendroglioma	III-IV	+	+	+	Left frontal	2777841	1105888	2.51	4.00	Died
14	50	Male	Anaplastic astrocytoma	III-IV	+	+	+	Left parietal	229039	106306	2.15	3.33	Died
15	25	Male	Anaplastic malignant astrocytoma	IV	+	+	+	Left temporal	92355	26466	3.49	5.625	Died
16	50	Male	Glioblastoma multiforme	IV	+	+	+	Right frontal	134936	39822	3.38	5.96	Died
17	57	Male	Glioblastoma multiforme	IV	+	+	+	Left medial temporal	1613826	973761	1.66	2.38	Died
18	50	Male	Glioblastoma multiforme	IV	NA	+	+	Right Parietal	318851	143058	2.23	4.00	Died
19	45	Male	Glioblastoma multiforme	IV	+	NA	+	Left medial temporal	230663	62451	3.69	6.33	Died
20	40	Female	Glioblastoma multiforme	IV	+	NA	+	Right postero-temporal	240063	68589	3.5	4.2	Died
21	50	Male	Brain metastases (unknown primary)	Metastases	+	+	+	Right frontal	141160	108125	1.30	1.40	Died
22	60	Female	Brain metastases (thyroid)	Metastases	+	+	+	Basisphenoid	3477065	1713355	2.03	2.56	Died
23	60	Female	Brain metastases (thyroid)	Metastases	+	NA	+	Left parietal and temporal	4159863	2753133	1.51	1.58	Died
24	40	Male	Brain metastases (lung)	Metastases	+	+	+	Multiple, frontal, parietal, occipital	439904	249372	1.76	2.66	Died
25	45	Female	Brain metastases (lung)	Metastases	+	NA	+	Right occipital	422105	201002	2.1	2.4	Died
26	55	Male	Infective	-	–	±	–	Left posterior parietal	-	-	1.0	1.0	Alive
27	70	Female	Cerebral infarction	-	+	NA	+	Left parietal	239121	114993	2.08	3.44	Alive
28	16	Female	Cerebral tuberculosis	-	NA	+	+	Multiple, parietal, occipital	169720	82100	2.06	2.40	Alive
29	50	Male	Gliosis (NSCLC)	-	±	NA	–	-	-	-	1.0	1.0	Died
30	60	Male	Oligodendroglioma, no recurrence	I	–	NA	–	-	-	-	1.0	1.0	Alive

A T/N ratio of <1.2 was considered as nonvisualization of the tumor. + – Positive for lesion; – – Negative for lesion; NA – Not available; NSCLC – Nonsmall cell lung cancer; WHO – World Health Organization; CT – Computed tomography; MRI – Magnetic resonance imaging; SPECT – Single photon emission computed tomography; T/N – Tumor to normal ratio

Group 5: It consisted of patients with nonneoplastic ICSOLs ($n = 5$).

Observations: Visual analysis

Normal subjects

Tc-99m GHA was performed in four normal subjects to study the physiological distribution of the two tracers. These patients were negative for ICSOLs clinically as well as on CECT/contrast-enhanced magnetic resonance (CEMR). The salient features of the normal distribution of Tc-99m GHA were as under.

Technetium-99m glucoheptonate single photon emission computed tomography

Postinjection initial dynamic 1 s perfusion frames showed the classical arterial phases with the visualization of the carotids and vertebral arteries followed by the arrival of the tracer at the circle of Willis and its branches namely, the two middle cerebral groups and the anterior cerebral group.

This arterial phase was followed by a capillary phase identified by its diffused pattern. This was followed by a venous phase with visualization of the cerebral venous sinuses, starting at the superior sagittal sinus which passed toward the cervical region. The venous clearance was slower with persistence of activity beyond 30 min of injection. A significant portion of patients who underwent SPECT at 1 h still showed the distribution of the radiopharmaceutical within these sinuses. These were more prominent in the posterior fossa at the confluence of the sinuses and could create problems in delineating small low-grade gliomas in the posterior fossa. However, these sinuses helped in the co-registration of images with their corresponding slices in CECT/CEMR.

Increased radiopharmaceutical uptake was seen in the highly vascular nasal mucosa as well as the skull base near the sella turcica from the activity within the cavernous sinuses.

Positive subjects

Tc-99m GHA SPECT was considered positive in those cases which showed focally increased tracer uptake within the brain parenchyma. The tracer uptake was evident in the areas of BBB breakdown and was more prominent in high-grade gliomas as compared to low-grade tumors or metastases. It was found that patients with high grade primary glial tumors like glioblastoma multiforme, anaplastic oligodendroglioma [Figure 3] as well as anaplastic astrocytomas [Figures 4 and 5] displayed distinctly higher T/N as well as Tmax/N ratio than low grade tumors and metastases baring a few cases like vestibular schwannoma [Figure 6] and two cases of glioblastomas with extensive necrosis (cases 17 and 18 of master table).

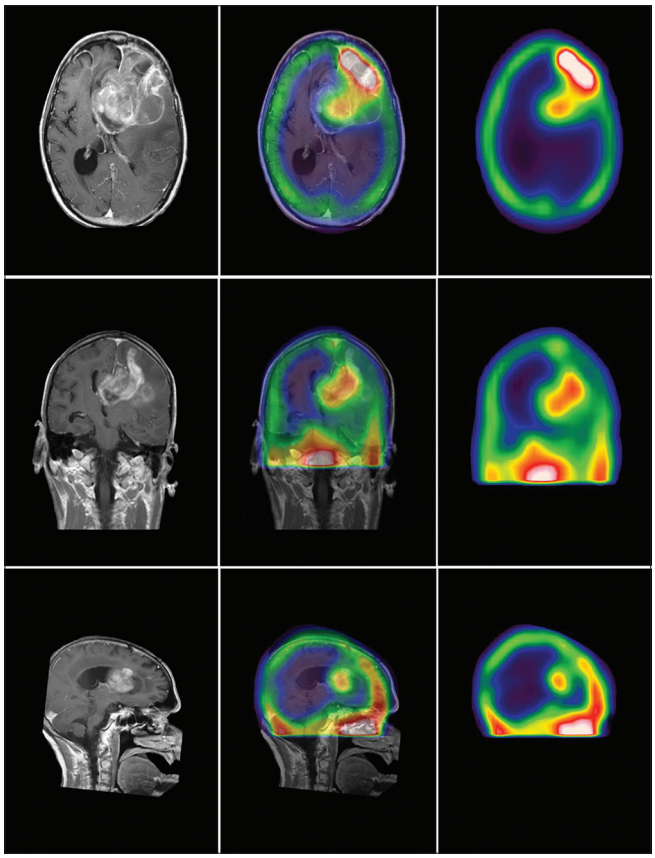

Figure 3: Anaplastic oligodendroglioma of the left prefrontal region. Case 13 master table

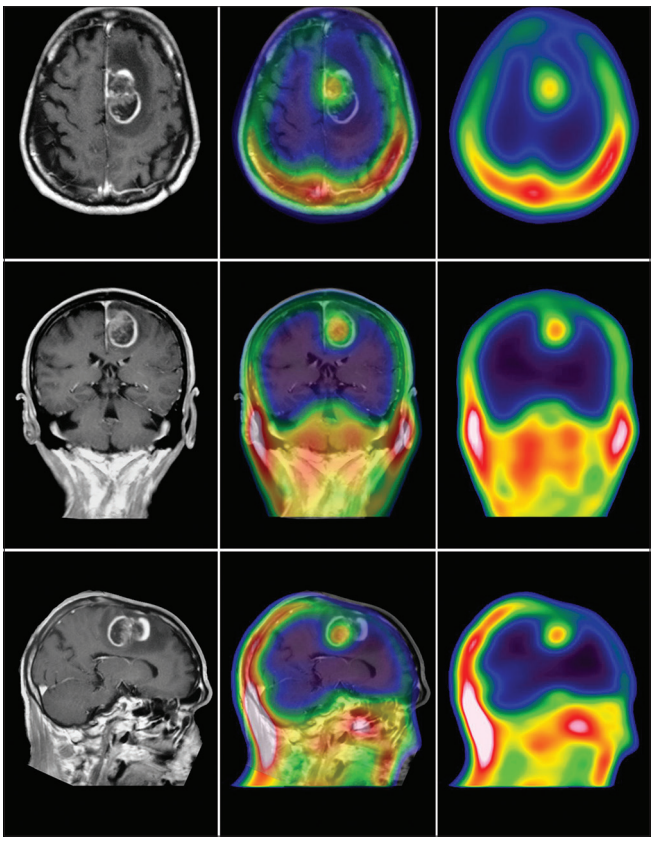

Figure 4: Anaplastic astrocytoma of the left high parietal region. Case 14 of master table

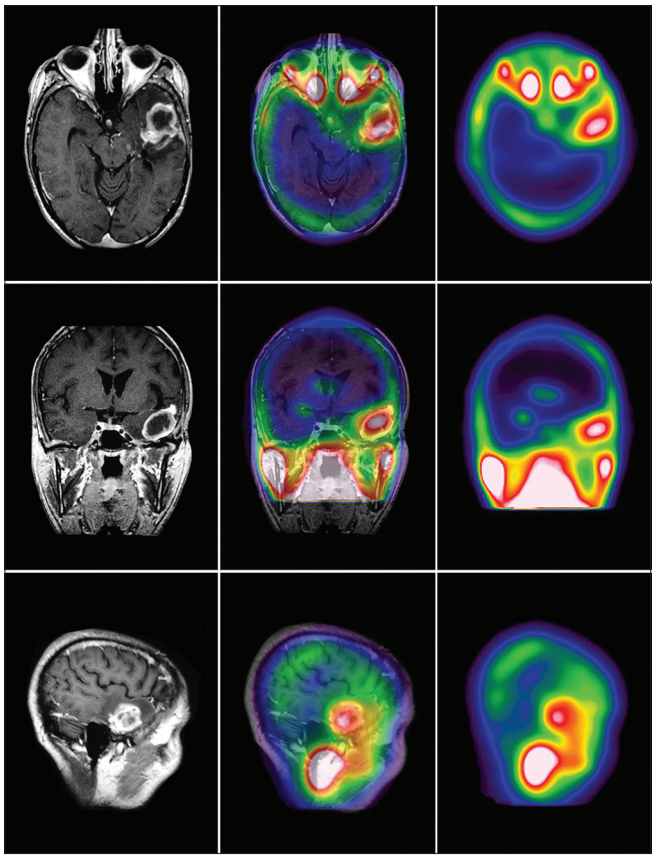

Figure 5: Anaplastic malignant astrocytoma of the left temporal region, Case 15 of master table

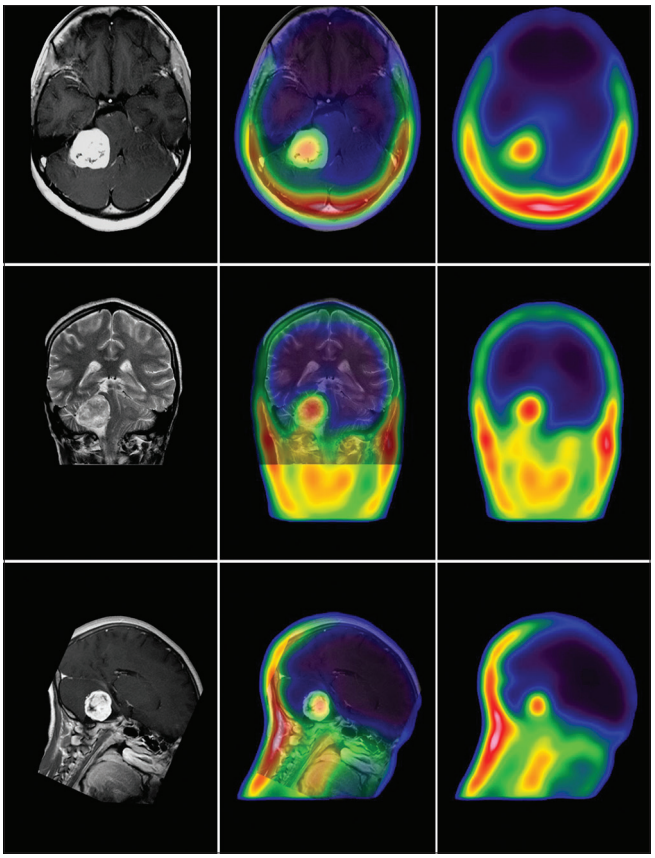

Figure 6: Vestibular schwanoma involving the right internal auditory meatus displaying higher T/N and Tmax/N ratios despite being benign. Case 7 of Master table

Contrast-enhanced computed tomography

Normal CECT was interpreted as negative for tumor when their Hounsfield unit values were close to cerebrospinal fluid density with no evidence of any mass effect, whereas lesions showing effacement of adjacent sulcal spaces (mass effect), with or without contrast enhancement were considered as positive for tumor. Low-grade tumors with an intact BBB were not detected as they did not show contrast enhancement. There was also no clear cut delineation between recurrent tumor and postradiotherapy changes.

Contrast-enhanced magnetic resonance imaging

Positive lesions on MRI typically appeared well-demarcated, hypointense or isointense relative to the brain on T1-weighted images and bright on T2-weighted images.

They invariably showed enhancement with gadolinium DTPA. There is associated mass effect, edema, hemorrhage, necrosis, or signs of increased intracranial pressure. Ring-like enhancement surrounding irregularly shaped foci presumed as necrosis was suggestive of glioblastoma.

Histological distribution of lesions

Of the 22 patients in which histological diagnosis was available, 22.7% (n = 5) had cerebral metastases, 22.7% (n = 5) had glioblastoma multiforme, 18.1% (n = 4) had astrocytoma, 18.1% (n = 4) had oligodendroglioma, 9.0% (n = 2) had meningioma, 4.5% (n = 1) [Figure 6] had vestibular schwannoma, and 4.5% (n = 1) had pituitary macroadenoma.

The most common histological entity was cerebral metastases, while glioblastoma was the most common primary brain tumor within the study group.

Correlation of technetium-99m glucoheptonate single photon emission computed tomography with contrast-enhanced computed tomography in relation to lesion detection

Of the 30 patients evaluated with Tc-99m GHA SPECT, 80% (n = 24) had undergone a CECT as the initial investigation while the rest had directly undergone a gadolinium-DTPA enhanced MRI. Four of these were controls and hence were not included in intermodality comparison.

Among these 20 patients, Tc-99m GHA SPECT showed concordant results in 95% (19) patients; in the only patient with discordant results, CECT could not differentiate between recurrent tumor and postradiotherapy gliosis while the SPECT study was negative, favoring the later diagnosis.

The CECT examinations were performed on 16 and 64 slice CT (Sensation, Siemens Corporation, Germany). Nonionic contrast agents were used in all the patients to detect contrast

enhancing lesions and corroborate the findings of SPECT as both the investigations are primarily based on the breakdown of the BBB in the vicinity of a mitotic lesion.

Even though the study group was small, the results obtained were comparable to data obtained during the 1980s with concordant results in 81% patients ($n = 209$) with false positive rates of SPECT and CECT being 0% and 0.5%, respectively. The false negative rates were calculated, respectively, at 2.4% and 6%.

On comparing the results of Tc-99m GHA SPECT with CECT, it was found that their correlation was significant ($P = 0.0001$).

At the same time, when significance was sought between CT and final diagnosis, it was also found to be significant ($P = 0.024$).

Correlation of technetium-99m glucoheptonate single photon emission computed tomography with magnetic resonance imaging in relation to lesion detection

MRI was regarded as the gold standard for preoperative localization of ICSOLs. In this study, gadolinium-DTPA enhanced MRI was performed in 57% ($n = 17$) of patients. The results were concordant with Tc-99m GHA SPECT in 82% ($n = 14$) of patients. It was discordant in three patients; two of whom (pituitary macroadenoma and low-grade oligodendroglioma) had lesions with an intact BBB as concurrently detected with a CECT which showed no contrast enhancement. Furthermore, the case with low-grade left frontal glioma had a negative single voxel magnetic resonance spectroscopy (MRS) with an insignificant choline to creatinine ratio of <2.0 (≈ 1, case 9 master table).

The third discordant patient had a tuberculoma which was reported as suspected metastases on MRI while MRS was nondiagnostic. SPECT, in this case, was negative suggestive of an infective pathology. The SPECT study was performed 6 months after the initial MRI. A follow-up CECT performed concurrently was negative being concordant with SPECT findings (case 9 master table).

Three of the patients had undergone an H1-MRS to delineate the chemical characteristics of the lesions. The results of MRS were concordant in one case (case 16 master table) and discordant in two. One of the three was proved correct on final (clinico-histopathological) diagnosis.

Correlation of technetium-99m glucoheptonate single photon emission computed tomography with final/ clinico-histopathological diagnosis

Histopathological examination was done in 22 patients. It included all patients in Groups 2, 3, and 4 and one patient with gliosis. Typically, a crush biopsy in the operation theater was followed by routine sections from tissue blocks by an experienced pathologist.

It was regarded as the gold standard for tumor characterization. The tumors were graded according to the most commonly used WHO, 2007 grading system.[6]

Four patients in Group 5 were treated on the grounds of infection/infarction and were followed up with periodical scans. Their condition improved in the following months, and subsequent scans (CECT/SPECT) showed marked improvement suggestive of nontumoral origin of the lesions.

The statistical parameters of Tc-99m GHA SPECT, final diagnosis, CECT/CEMR are described in Tables 2-6.

Correlation of technetium-99m glucoheptonate indices with histopathological grade (World Health Organization classification)

As explained earlier, semi-quantitative analysis was performed within the study groups using the Tc-99m GHA indices, i.e., T/N and T_{max}/N ratios.

Table 2: Comparison of CECT diagnosis with final diagnosis, HPE/clinical (n=20)

	HPE/FD positive	HPE/FD negative	Total
CECT positive	15	2	17
CECT negative	1	2	3
Total	16	4	20

True positive=15, True negative=2, False positive=2, False negative=1; Sensitivity=93.8%, Specificity=50%, Positive predictive value=88.2%, Negative predictive value=66.7%. CECT – Contrast-enhanced computed tomography; HPE/FD – Histopathological examination or final clinical diagnosis

Table 3: Head to head comparison of Tc-99m SPECT diagnosis with CECT diagnosis (n=20)

	True positive	True negative	False positive	False negative	Total
SPECT	15	3	1	1	20
CECT	15	2	2	1	20

SPECT sensitivity=93.8%, Specificity=75.0%, Positive predictive value=93.8%, Negative predictive value=75.0%; CECT sensitivity=93.8%, Specificity=50.0%, Positive predictive value=88.2%, Negative predictive value=66.7%. CECT – Contrast-enhanced computed tomography; SPECT – Single photon emission computed tomography; Tc-99m – Technetium-99m

Table 4: Comparison of CEMR diagnosis with final diagnosis, HPE/clinical (n=17)

	HPE/FD positive	HPE/FD negative	Total
CEMR positive	15	2	17
CEMR negative	0	0	0
Total	15	2	17

True positive=15, True negative=0, False positive=0, False negative=2; Sensitivity=100%, Positive predictive value=88.23%. CEMR – Contrast-enhanced magnetic resonance; HPE/FD – Histopathological examination or final clinical diagnosis

Table 5: Head to head comparison of Tc-99m SPECT diagnosis with CEMR diagnosis (n=17)

	True positive	True negative	False positive	False negative	Total
SPECT	13	1	1	2	17
CEMR	15	0	2	0	17

SPECT Sensitivity=86.67%, Specificity=50.0%, Positive predictive value=92.86%, Negative predictive value=33.33%; CEMR sensitivity=100%, Positive predictive value=88.23%. CEMR – Contrast-enhanced magnetic resonance; SPECT – Single photon emission computed tomography

Statistical analysis consisted of one-way analysis of variance (ANOVA) within five groups.

ANOVA showed a significant difference ($P = 0.0001$) between the T/N GHA as well as T_{max}/N GHA indices between high- and low-grade tumor groups. These can be visualized in Figure 7.

Correlation between tumor to normal and T_{max}/N

A correlation was sought between T/N and T_{max}/N GHA indices. This would give an insight into the relationship of averaged tumor counts within multiple transverse sections as depicted in the frame activity curve (i.e. T/N) to the absolute comparison of T/N ratios in the frame showing the highest concentration of tracer within the tumor (T_{max}/N).

Both the indices showed similar results with regard to differentiating all grades of ICSOLs from high-grade (WHO III/IV) primary brain tumors.

The statistical results confirm a significant relationship between these two indices, and hence either of them can be used in differentiating high-grade tumors from low-grade ones. However, the standard deviation is smaller in case of T/N GHA index.

T_{max}/N GHA index describes the most malignant part of the tumor hence has higher absolute value than the T/N GHA index. It also corresponds to the area with the highest BBB breakdown.

Table 6: Comparison of Tc-99m GHA SPECT diagnosis with final/histopathological diagnosis

	HPE/FD positive	HPE/FD negative	Total
SPECT positive	19	2	21
SPECT negative	2	3	5
Total	21	5	26

True positive=19, True negative=3, False positive=2, False negative=2; Sensitivity=90.48%, Specificity=60.0%, Positive predictive value=90.48%, Negative predictive value=60%. SPECT – Single photon emission computed tomography; Tc-99m GHA – Technetium-99m glucoheptonate; HPE/FD – Histopathological examination or final clinical diagnosis

Discussion

Cancers of all forms cause 9% of deaths throughout the world. In developed countries cancer is the second most leading cause of death, next only to cardiovascular disease. On the other hand it stands as the fourth largest cause of death in developing countries, accounting for 6% of all deaths.[6]

In the past, tumors of the central nervous system (CNS) were regarded as a relatively rare phenomenon. With the advent of newer modalities of imaging, it became clear that they accounted for 1.2% of all autopsied deaths and 9% of all neoplasms.[6]

Gliomas are CNS tumors derived from the cells believed to be of glial origin. Constituting 45–55% of all primary intracranial neoplasms, they are the most common primary CNS tumors. In spite of this, only a quarter of intracranial mitotic lesions represents primary brain tumors the rest being metastatic in origin. Despite this fact as well as their relative scarcity, adult glial tumors have a significant public health impact.[6]

Systematic classifications in a modern sense essentially began with the histogenetic system of Bailey and Cushing; however, the first major alternative to a strict histogenetic scheme was offered by Kernohan *et al*. The fully developed Kernohan classification divided each of the

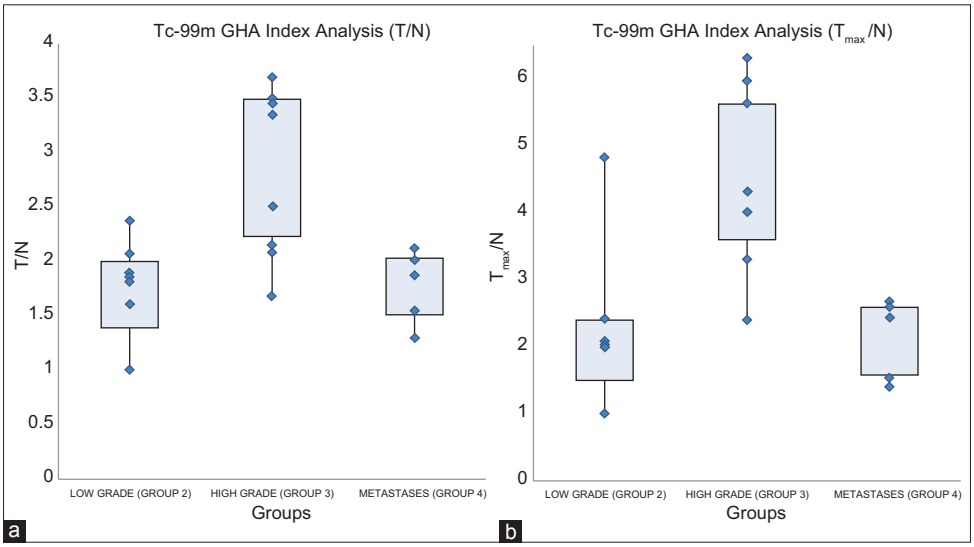

Figure 7: Bar diagram showing the percentage histological distributions of the patients in the study. (a) The above table shows that there was a statistically significant difference between the tumor to normal ratios of high- and low-grade gliomas on technetium-99m glucoheptonate single photon emission computed tomography. (b) The above table shows that there was a statistically significant difference between the tumor (maximum intensity pixel) to normal (T_{max}/N) ratios of high- and low-grade gliomas on technetium-99m glucoheptonate single photon emission computed tomography

major glioma types, astrocytoma, oligodendroglioma, and ependymoma into four grades of increasing malignancy. Ringertz offered a conceptually similar scheme with one important difference that instead of four, it was a three tier classification.[6]

The WHO classification also adopted the essentials of this scheme but separated pilocytic and a few other "special" subtypes as Grade I, used the three Grades II, III, and IV as synonyms for astrocytoma, anaplastic astrocytoma, and glioblastoma multiforme, respectively.[6,7]

Since the advent of brain imaging in the first half of the last century, there has been development in CNS imaging by leaps and bounds, more so in the last three decades. The development of SPECT and CT followed by MRI and positron emission tomography (PET)-CT has revolutionized the preoperative localization and grading of ICSOLs.

Functional imaging of the brain began in the late 1940s. It involved static imaging using I-131 labeled human serum albumin. The introduction of Hg-203 labeled chlormerodrin by Bender and Blau and the subsequent development of Hg-197 labeled chlormerodrin replaced radioiodinated albumin as the agent of choice for brain scanning. Imaging was performed using rectilinear scanners and early anger cameras and was physiologically based on the increased permeability of the BBB.[8,9]

With the introduction of Tc-99m pertechnetate brain scanning by Harper and the availability of the Mo-99/Tc-99m generator from the Brookhaven National Laboratory, Tc-99m pertechnetate scan became a well-established and safe method for the *in vivo* evaluation of intracerebral lesions.[9,10]

Although it had a favorable physical and imaging characteristics, it also had its own shortcomings. About 15–20% of brain tumors were not detected. It also had problems of physiological uptake in the choroid plexus; however, this could be minimized by blocking the uptake with perchlorates prior to the study.[10-22]

Witcofski *et al*. studied 1000 patients for the localization of intracranial lesions using Tc-99m pertechnetate and a rectilinear scanner and found that it had a sensitivity of 81.5%; they also concluded that it could be also used in nonneoplastic conditions such as arteriovenous malformations, hematomas, vascular occlusions, and abscess. They concluded that the Tc-99m brain scan was very valuable as a screening test for intracranial lesions.[12]

Bernstein and Hoffer studied 92 sequential positive scans of 67 patients at 30 min and 3 h after premedication with 1 g perchlorate. He compared the relative radioactivity in the lesion with the rim radioactivity and found that in more than 80% of calvarial lesions, the radioactivity tended to decrease between early and delayed views whereas in more than 90% of the intracranial lesions tended to increase. They concluded that by doing early and delayed imaging, it was possible to achieve a higher specificity than either study performed alone.[13]

Schwartz and Tator stated that despite the excellent physical characteristics of Tc-99m pertechnetate, its sensitivity was poor. They studied 52 patients undergoing craniotomy for intracranial mass lesions who have injected 10 min to 4 h before the procedure. They found that malignant meningiomas were the most radioactive while benign astrocytomas were the least, with metastases, pituitary tumors, and other gliomas being intermediate in uptake. Surprisingly, they found a very high uptake in acoustic neuromas. On the contrary, intracerebral hematomas showed a very low uptake. They also observed that within an individual histological type the uptake increased with increasing grade of malignancy.[14]

These shortcomings heralded the use of newer Tc-99m labeled radiopharmaceuticals in brain scanning, the most prominent of these being Tc-99m DTPA and Tc-99m GHA. Both of these were established renal agents and did not penetrate the intact BBB.[14]

Early studies showed improved target to nontarget ratios, especially on delayed scans (1–4 h) as well as no choroid plexus uptake.[23]

Later tracers, such as thallium-201 in the late 70's and technetium-based thallium analogs in the mid-80's, were shown to accumulate in viable myocardium and became increasingly used for tumor imaging.

Kaplan *et al*. demonstrated the superiority of thallium-201 scans over Tc-99m GHA, Ga-67, and CT in gliomas. They studied 29 patients over an interval of 18 months. They concluded that thallium-201 showed the best correlation with viable tumor; Tc-99m GHA could not differentiate between tumor necrosis and edema; Ga-67 showed lower uptake than both and CT could not routinely differentiate between fibrotic, nonfibrotic, necrotic, and neoplastic tissue.[24]

Later studies by Kim *et al*. have proved that brain SPECT with Tc-99m GHA is a simple but very sensitive method in detecting brain tumors and has some value in preoperative characterization of tumor types thereby having potential to be used as a screening test for brain tumors.[25]

Barai *et al*. reiterated that the use of Tc-99m GHA was discouraged previously as it was believed to be inferior to other CNS tumor labeling agents because of its dependence on the disruption of the BBB rather than active extraction of the tracer in relation to tumor metabolism, which was not true.[26]

Mittal *et al*. have added that it is as sensitive as MRI in detecting glial tumors and the modality can help in grading of glial tumors, especially Grade I/II from III/IV.[27]

Barai *et al*. further established that Tc-99m GHA is a reliable diagnostic modality in medulloblastomas where other

radiopharmaceuticals did not concentrate. They described that the only shortcoming of Tc-99m GHA SPECT had been its low sensitivity in detecting posterior fossa tumors as studied. Tc-99m GHA shows intense physiological uptake in nasal mucosa, and large intracranial venous sinuses also retain a significant amount of radioactivity.[28]

Ashok *et al*. remarked that Tc-99m GHA brain SPECT allows a good visualization of tumor margins. There was a lower mean value for Tc-99m GHA index in high-grade tumors versus low-grade tumors.[29]

Tc-99m GHA was later described by Thomas *et al*. as an invaluable tool in the postoperative evaluation of patients undergoing radiotherapy in the determination of recurrent tumor from postradiotherapy gliosis.[30]

Barai *et al*. confirmed the findings of Thomas and reiterated its value in postradiotherapy scenarios in the pediatric age group.[31,32]

Ray *et al*. described nuclear imaging to be reliable in describing neoplastic from nonneoplastic ring-enhancing lesions.[33]

Jaiswal *et al*. observed the Tc-99m GHA SPECT has a high specificity for neoplastic tissues as compared to nonneoplastic lesion determining its sensitivity and specificity being 97.62% and 100%, respectively.[34]

Santra *et al*. studied the use of Tc-99m GHA in the imaging of brain tumors in 85 patients of histopathologically proven glioma with a clinical suspicion of recurrence using Tc-99m GHA SPECT and MRI. Tc-99m GHA SPECT showed sensitivity, specificity, and accuracy of Tc-99m GHA SPECT were 86.5%, 96.5%, and 89.4%, respectively, whereas those of CEMR were 94.6%, 24.1%, and 70.5%, respectively. Thirty patients had intermodality discordance, with Tc-99m GHA SPECT being correct in 23 of them.[35,36]

In another study by Santra *et al.* performed to compare the performance of Tc-99m GHA SPECT and F-18 FDG PET-CT for detection of tumor recurrence in patients of glioma they found that Tc-99m GHA had a sensitivity, specificity and accuracy of 85%, 97% and 89% respectively whereas those for F-18 FDG PET-Ct were 70%, 97% and 80% respectively. On histopathological subgroup analysis, Tc-99m GHA SPECT performed better than F-18 FDG PET-CT in all grades except for Grade II gliomas, where both were equally effective. In all, 15 patients in this series had intermodality discordance, with Tc-99m GHA SPECT being correct in 13 of them.[37]

In another recent study, Karunanithi *et al*. compared the diagnostic accuracies of Tc-99m GHA SPECT-CT with F-18 fluorodopa (F-18 FDOPA) PET/CT in 30 patients with suspicion of recurrent glioma. Sensitivity, specificity, and accuracy were 86.4%, 62.5%, and 80% for Tc-99m GHA SPECT-CT and 100%, 87.5%, and 96% for F-18 FDOPA PET-CT, respectively. No significant difference was found between them overall ($P = 1.00$) as well as for low-grade ($P = 0.250$) or high-grade tumors ($P = 0.50$). The authors concluded that Tc-99m GHA SPECT-CT could be used as a low-cost alternative to F-18 FDOPA PET/CT for recurrent glioma.[38]

In the same context, Jacob *et al*. showed the F-18 FDOPA PET-CT was more reliable than F-18 FDG PET-CT or N-13 ammonia PET-CT in evaluating brain tumors, thereby putting Tc-99m GHA in the same league of radiotracers even though it is more economical and widely available than the other PET radiotracers.[39]

In our study, the main aim was to evaluate an economically viable physiological agent-like Tc-99m GHA, a saccharide [Figure 8], aptly nicknamed as the "poor man's FDG" in the semi-quantitative evaluation of brain tumors.

The results showed that this radiopharmaceutical can significantly demonstrate high-grade (WHO Grade III/IV) gliomas from low-grade (WHO Grade I/II) gliomas as well as from metastases and nontumoral ICSOLs.

It showed a sensitivity of 93.8%, a specificity of 75%, and a positive predictive value of 93.8% and a negative predictive value of 75% as compared to 93.8%, 50%, 88.2%, and 66.7%, respectively, for CECT. This is in concordance with results obtained in the 1980s in 209 patients. The study had showed that the false positive rates of SPECT and CT were 0% and 0.5%, respectively while the false negative rates were 2.4% and 6%, respectively. To date, this similar sensitivity for detection of tumoral ICSOLs has never been challenged.[5]

MRI was considered as a gold standard for the preoperative detection of tumors only two statistical parameters were obtained in a head to head comparison. When compared to CEMR, SPECT showed a sensitivity of 86.67%, a specificity of 50%, a positive predictive value of 92.86% and a negative predictive value of 33.33% as compared to a sensitivity of 100% and a positive predictive value of 88.23% for CEMR.

Qualitatively, on imaging alone, Tc-99m GHA could not differentiate between tumoral and nontumoral ring-enhancing lesions. However one could provide a differential diagnosis based on pattern of uptake which differed between tumor and

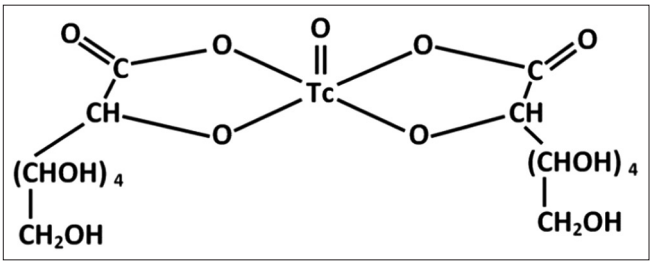

Figure 8: Technetium-99m glucoheptonate molecular structure

stroke or by adding complementary investigations like blood/CSF examinations in case of tuberculosis.

This was probably because of the dependency of these radiopharmaceuticals to accumulate in the areas of BBB breakdown. There are, however, other mechanisms of tracer uptake such as increased vascularity, metabolism, active transport. However, these latter mechanisms have a lesser contribution in tumoral uptakes at 1–2 h postinjection of the radiopharmaceutical.

The same may be considered if delayed imaging is planned for 4–9 h postinjection, such studies though exciting are logistically difficult to carry out in a busy Nuclear Medicine Department. They also have inherently poorer counting statistics due to radioactive decay of the radiopharmaceutical which makes it necessary to increase acquisition times which in turn increase the chances of motion artifacts.

Interestingly, it was noted that some low-grade tumors such as vestibular schwannoma (case 7 of master table) showed an intense uptake of Tc-99m GHA ($T_{max}/N = 4.82$) however T/N ratios fell within the range of low-grade tumors ($T/N = 1.74$). On the other hand, some high-grade tumors showing central necrosis such as glioblastomas (case 17 of master table) showed much lower Tc-99m GHA indices. In such instances, using manually generated contoured ROIs should be used around the rim of the tumor which will physiologically correspond to the active tumoral tissue.

Previous studies done with Tc-99m GHA were mostly done in the 1970s in an era of planar imaging over the years the introduction of SPECT and improvements in instrumentation have made SPECT a powerful tool in demonstrating physiology. Even though it has a poorer resolution (7–10 mm) when compared to PET, it has the advantages of availability, cost-effectiveness, and the ability to use multiple radiopharmaceuticals in the same study.

The limitations of this study were the inability of performing SPECT with low-energy high-resolution and low-energy ultra-high resolution collimators as well as fan beam collimators, due to lack of availability which would have increased the resolution to subcentimeter levels and decreased interference of partial volume effect.

The small number of cases was another important limitation so was the inability to compare early (1–2 h) and delayed images of each patient (4–9 h) or establishment of retention indices due to logistical reasons.

Another technical limitation was the inability to generate a three dimensional ROI conforming to the non geometrical shapes of the tumoral lesions which would account in the histological milieu of the tumor (proliferative areas, edema and necrosis). This parameter would have been a better reflection of the actual tumor volume, and hence a better index could have been calculated. Nevertheless, this study provides a new technique in calculating Tc-99m GHA index taking into account multiple sections rather than one. This method yields consistent results with a small standard deviation.

These limitations need to be worked out in subsequent studies with this radiopharmaceutical.

Conclusions

In summary, the results of this study suggest that Tc-99m GHA SPECT is capable of distinguishing high-grade gliomas from low-grade gliomas as well as metastases.

It also suggests that it has a high sensitivity and specificity in localizing ICSOLs and can be used in patients who cannot undergo CECT/CEMR due to contraindications or if the waiting lists for such tests is long.

Apart from this, it has an invaluable contribution in the follow-up of patients who have undergone surgery followed by radiotherapy as a complementary investigation in differentiating recurrent tumor from postradiotherapy gliosis.

However, it cannot differentiate nontumoral lesions causing a breakdown of the BBB from low-grade tumors or metastases, on imaging alone.

Financial support and sponsorship
Nil.

Conflicts of interest
There are no conflicts of interest.

References

1. Finger S, Origins of Neuroscience. Oxford University Press; Reprint edition 2001. p. 14.
2. Thrall JH, O'Malley JP, Ziessman HA, Nuclear Medicine: The Requisites: 3rd ed. 2006. p. 419-49.
3. Ell PJ, Gambhir SS. Nuclear Medicine in Clinical Diagnosis and Treatment. 3rd ed. Churchill Livingstone; 2004. p. 1235-9.
4. Chang LT. A method for attenuation correction in radionuclide computed tomography. IEEE Trans Nucl Sciences;NS25:638-43.
5. Del Sole A, Moncayo R, Tafuni G, Lucignani G. Position of nuclear medicine techniques in the diagnostic work-up of brain tumors. Q J Nucl Med Mol Imaging 2004;48:76-81.
6. Govindan R. The Washington Manual of Oncology. 2nd ed. Wolters Kluwer, Lippincott William & Wilkins First Reprint; 2008. p. 104-17
7. Louis DN, Ohgaki H, Wiestler OD, Cavenee WK, editors. WHO Classification of Tumors of the Central Nervous System. Lyon: IARC; 2007.
8. Di Chiro G, Ashburn WL, Grove AS. Which radioisotopes for brain scanning? Neurology 1968;18:225-36.
9. Di Chiro G. RISA encephelography and conventional neurologic methods. Acta Radiologica (Stockholm, Norstedt and Soner), 1961;Suppl (2001).

10. Harper PV, Beck RN, Charleston DB, Lathrop KA. Optimization of a scanning method using 99mTc. Nucleonics 1964;22(1):50-4.
11. Harper PV, Lathrop KA, Jiminez F, Fink R, Gottschalk A. Technetium 99m as a scanning agent. Radiology 1965;85:101-9.
12. Witcofski RL, Maynard CD, Roper TJ. A comparative analysis of the accuracy of the technetium-99m pertechnetate brain scan: Follow-up of 1000 patients. J Nucl Med 1967;8:187-96.
13. Bernstein J, Hoffer PB. Use of the delayed brain scan in differentiating calvarial from cerebral lesions. J Nucl Med 1974;15:681-4.
14. Schwartz ML, Tator CH. Shortcomings of 99m Tc-pertechnetate as a tracer for brain tumor detection as shown by well counting of human brain tumors and a mouse ependymoblastoma. J Nucl Med 1972;13:321-7.
15. Quinn JL 3rd. Tc-99m pertechnetate for brain scanning. Radiology 1965;84:354-5.
16. Kuhl DE, Pitts FW, Sanders TP, Mishkin MM. Transverse section and rectilinear brain scanning with Tc-99-m pertechnetate. Radiology 1966;86:822-9.
17. Webber MM. Technetium 99m normal brain scans and their anatomic features. Am J Roentgenol Radium Ther Nucl Med 1965;94:815-8.
18. Tauxe WN, Thorsen HC. Cerebrovascular permeability studies in cerebral neolasms and vascular lesions: Optimal dose-to-scan interval for pertechnetate brain scanning. J Nucl Med 1969;10:34-9.
19. Miller MS, Simmons GH. Optimization of timing and positioning of the technetium brain scan. J Nucl Med 1968;9:429-35.
20. Levy LM, Siddiqui N, Siverstein S, Hyams C, 13. Technetium-99m brain scan: Non visualized lesions at early intervals. J Nucl Med 1966;7:382.
21. Ramsey RG, Quinn JL 3rd. Comparison of accuracy between initial and delayed 99m Tc-pertechnetate brain scans. J Nucl Med 1972;13:131-4.
22. Schwartz ML, Tator CH. Shortcomings of Tc-99m pertechnetate as a tracer for brain tumor detection as shown by well counting of human brain tumors and a mouse ependymoblastoma. J Nucl Med 1971;13:321-7.
23. Waxman AD, Tanacescu D, Siemsen JK, Wolfstein RS. Technetium-99m-glucoheptonate as a brain-scanning agent: Critical comparison with pertechnetate. J Nucl Med 1976;17:345-8.
24. Kaplan WD, Takvorian T, Morris JH, Rumbaugh CL, Connolly BT, Atkins HL. Thallium-201 brain tumor imaging: A comparative study with pathologic correlation. J Nucl Med 1987;28:47-52.
25. Kim JH, Lee SH, Lim SM, Hong SW. Department of neurosurgery, Korea cancer center hospital, Seoul, Korea. Evaluation of brain SPECT using Tc-99m GHA and Tc-99m HMPAO in brain tumors. J Korean Neurosurg Soc 1989;18:706-15.
26. Barai S, Bandopadhayaya GP, Julka PK, Kale SS, Kumar R, Malhotra A, *et al*. Evaluation of Tc99m-glucoheptonate for SPECT functional imaging of medulloblastoma. J Clin Neurosci 2005;12:36-8.
27. Mittal BR, Bhattacharya A, Singh B. 2005 ASCO annual meeting 99mTc-GHA brain SPECT in the evaluation of brain tumors. 2005 ASCO annual meeting, Abstract No: 1549. J Clin Oncol 2005;23, (Suppl 1):1549.
28. Barai S, Bandopadhayaya GP, Naik K, Haloi AK. Department of Nuclear Medicine, AIIMS, New Delhi. Is brain SPECT a suitable modality for evaluation of postradiotherapy posterior fossa brain tumours? A comparative evaluation with contrast enhanced computed tomography. J Indian Med Assoc 2004;102:477-9, 486.
29. Ashok KR, Niranjan K, Singh SK, Pathak A, Mittal BR, Radotra BD, *et al*. Comparison between contrast-enhanced magnetic resonance imaging and technetium 99m glucohepatonic acid single photon emission computed tomography with histopathologic correlation in gliomas. J Comput Assist Tomogr 2006;30:723-33.
30. Thomas EJ, Bal CS, Barai C, Bandopadhyay GP, Julka PK. 99mTc Glucoheptonate brain SPECT: An invaluable tool in the management of post-operative patients with primary brain tumors receiving radiotherapy; correlative study with CT, MRI and clinical outcome in 140 patients. J Nucl Med 2002;43:249.
31. Barai S, Bandopadhayaya GP, Julka PK, Naik KK, Haloi AK, Kumar R, *et al.* Role of Tc-glucoheptonic acid brain single photon emission computed tomography in differentiation of recurrent brain tumour and post-radiation gliosis. Australas Radiol 2004;48:296-301.
32. Barai S, Bandopadhayaya GP, Julka PK, Naik K, Haloi A, Malhotra A. Department of nuclear medicine, AIIMS, New Delhi: Evaluation of tumor viability in Post radiation therapy pediatric brain tumors with ^{99m}Tc glucoheptonate single photon emission computed tomography (SPECT) Mcgill J Med Can 2005.
33. Ray S, Kundu B, Kundu S, Roy S, Sharma SK. Distinguishing neoplastic and non-neoplastic ring enhancing lesions of the brain detected in CT and/or MRI with the help of correlative nuclear imaging. Neuroradiol Head Neck Imaging 2001;12:189-95.
34. Jaiswal S, Barai S, Rajkumar, Gambhir S, Ora M, Mahapatra AK. Evaluation of intracranial space-occupying lesion with Tc99m-glucoheptonate brain single photon emission computed tomography in treatment-naïve patients. J Postgrad Med 2009;55:180-4.
35. Santra A, Kumar R, Sharma P. Use of 99m-technetium-glucoheptonate as a tracer for brain tumor imaging: An overview of its strengths and pitfalls. Indian J Nucl Med 2015;30:1-8.
36. Santra A, Sharma P, Kumar R, Bal C, Kumar A, Julka PK, *et al.* Comparison of glucoheptonate single photon emission computed tomography and contrast-enhanced MRI in detection of recurrent glioma. Nucl Med Commun 2011;32:206-11.
37. Santra A, Kumar R, Sharma P, Bal C, Julka PK, Malhotra A. Detection of recurrence in glioma: A comparative prospective study between Tc-99m GHA SPECT and F-18 FDG PET/CT. Clin Nucl Med 2011;36:650-5.
38. Karunanithi S, Bandopadhyaya GP, Sharma P, Kumar A, Singla S, Malhotra A, *et al.* Prospective comparison of (99m) Tc-GH SPECT/CT and (18) F-FDOPA PET/CT for detection of recurrent glioma: A pilot study. Clin Nucl Med 2014;39:e121-8.
39. Jacob MJ, Pandit AG, Jora C, Mudalsha R, Sharma A, Pathak HC. Comparative study of (18) F-DOPA, (13) N-Ammonia and F18-FDG PET/CT in primary brain tumors. Indian J Nucl Med 2011;26:139-43.